RSC Advances

This article can be cited before page numbers have been issued, to do this please use: M. Norouzi, A. Ghorbani-Choghamarani and M. Nikoorazm, *RSC Adv.*, 2016, DOI: 10.1039/C6RA19776K.

ROYAL SOCIETY OF CHEMISTRY

www.rsc.org/advances

RSC Advances

View Article Online
DOI: 10.1039/C6RA19776K

ARTICLE

gReceived 00th January 20xx,
Accepted 00th January 20xx

DOI: 10.1039/x0xx00000x
www.rsc.org/

Heterogeneous Cu(II)/L-His@Fe_3O_4 nanocatalyst: a novel, efficient and magnetically-recoverable catalysts for organic transformations in green solvents

Masoomeh Norouzi , Arash Ghorbani-Choghamarani ,* Mohsen Nikoorazm

A novel, efficient and green Cu(II)/L-His@Fe_3O_4 catalyst has been applied successfully in the synthesis of heterocyclic compounds. The resulted catalyst were used in the synthesis of 2,3-dihydroquinazolin-4(1H)-ones, polyhydroquinolines and 2-amino-6-(arylthio) pyridine-3,5-dicarbonitriles as biologically interesting compounds. The present research is focused on investigation of recycling, reusability and stability of the catalyst in the phase reaction. The Cu (II)/L-His@Fe_3O_4 catalyst was used at least six times with comparable activities to that of fresh catalyst. The chemical composition and the structure of the catalyst were analysed by TGA/DTG, EDS, XRD, VSM, FT-IR and SEM.

Introduction

Metal–organic interfaces with biologically active molecules are important issues in biocatalysts, biocompatibility, and biosensors. Histidine and its peptides are interesting for possible applications, and one example is the electrochemical detection of metal ions [1].

It is well-known that histidine (2-amino-3-(4-imidazolyl) - propanoic acid, His) is an essential amino acid for human growth and repair of tissues and acts as a neurotransmitter in the central nervous of mammals [2-3]. The imidazole side chain of histidine can serve as a coordinating ligand in the metal ions transmission in biological bases [4] and was detected in the active sites of certain enzymes (**Scheme 1**) [5].

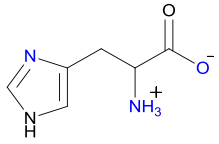

Scheme 1. A potential tridentate ligand, L-histidine.

Copper is an essential metal element for all living organisms [6-7]. Since the discovery of Copper (II)–L-Histidine species in human blood (Sarkar et al., 1966), extensive research has been carried out to determine its role in copper uptake into cells [8-11].

The solid state monocrystal X-ray structural analysis of this complex shows four coordinate square-planar arrangement around copper ion with nitrogen and oxygen atoms in trans coordination (**Scheme 2**) [12].

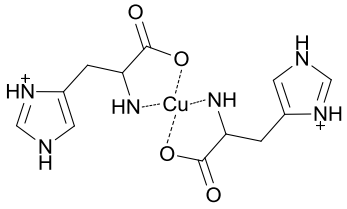

Scheme 2. The structure of the Cu(L-His)$_2$ complex.

Immobilization of Copper (II)–L-Histidine onto solid surface is the key step for creating a recoverable and reusable catalyst or reagent

A. Ghorbani-Choghamarani, Department of Chemistry, Faculty of Science, Ilam University, P.O. Box 69315516, Ilam, Iran; Tel/Fax: +98 841 2227022; E-mail address: arashghch58@yahoo.com or a.ghorbani@mail.ilam.ac.ir

In this context, magnetic nanoparticles (MNPs) materials have been efficiently used as environmentally friendly solid supports for immobilizing homogeneous catalysts

The main advantage of this catalytic system is high surface area and low toxicity, potential towards applications in various fields such as uses in disciplines including physics, biomedicine, biotechnology, material science and catalyst support. In addition the magnetic nanoparticles can be efficiently isolated from the reaction medium by magnetic separation [13-15].

2,3-Dihydroquinazolin-4(1H)-ones and polyhydroquinolines are an important group of nitrogen containing heterocyclic that have attracted much attention because of their diverse therapeutic and pharmacological properties, such as vasodilator, hepatoprotective, antiatherosclerotic, antidefibrillatory, antipyretic, analgesic [16-23].

The pyridine ring systems represent the major class of heterocycles and their analogues show diverse biological and physiological activities [24]. Among the pyridine derivatives, 2-amino-6-(arylthio) pyridine-3, 5-dicarbonitrile is a privileged scaffold for developing pharmaceutical agents because various compounds with this structural motif display significant and diverse biological activities. Compounds with 2-amino-3,5-dicarbonitrile-6-thio-pyridines ring system exhibit diverse pharmacological activities and are useful as anti-prion, anti-hepatitis B virus, anti-bacterial, and anticancer agents and as potassium channel openers for treatment of urinary incontinence [25-29].

In this communication, we report preparation and characterization of a novel, efficient and green Cu(II)/L-His@Fe_3O_4 catalyst for the synthesis of 2,3-dihydroquinazolin-4(1H)-ones, polyhydroquinolines and 2-amino-6-(arylthio) pyridine-3,5-dicarbonitrile through MCRs. Furthermore, the catalyst can be easily separated with an external magnet without using extra organic solvents or more filtration steps. Thus, the technology is green and solves the problems associated with mass transfer and recycling in multi-component reactions.

Results and discussion

The process of Cu(II)/L-His@Fe_3O_4 synthesis is schematically described in Scheme 3.

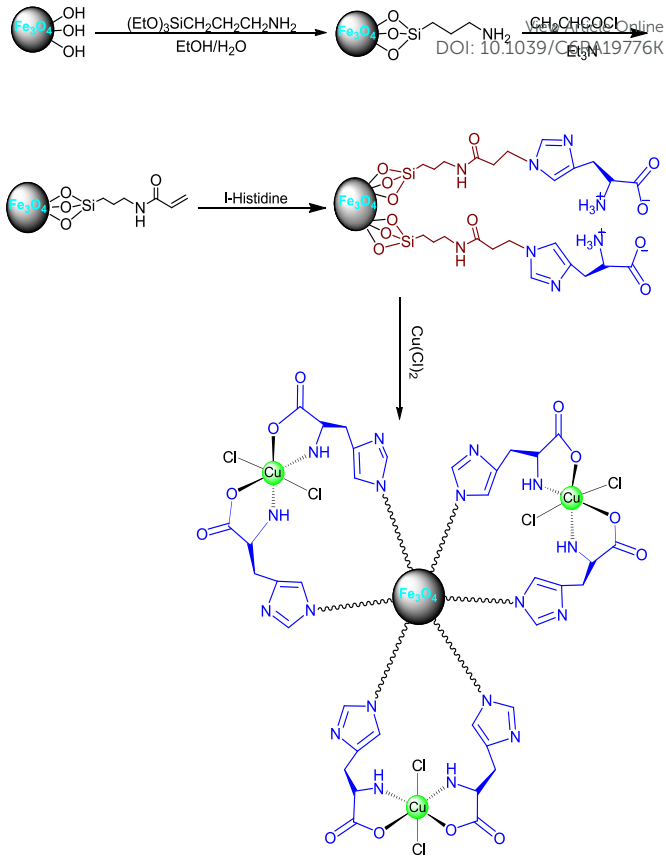

Scheme 3. Synthesis of Cu(II)/L-His@Fe_3O_4.

Characterization of the Cu(II)/L-His@Fe_3O_4

The catalyst has been characterised using a number of different complementary techniques.

FTIR spectra of Fe_3O_4 nanoparticles (a), functionalized Fe_3O_4 (b-e) and recovered catalyst (f) are shown in Fig. 1. Typical peaks at 573 cm^{-1} and 3500-2800 cm^{-1} originated from stretching vibration of the Fe–O and O-H (Fe_3O_4 nanoparticles Fig. 1. a). The C–H and N–H vibration bands in the 2922–2852 cm^{-1} and 1650–1500 cm^{-1} region were found in the FTIR spectra of Fig.1b, indicating the successful attachment of APTES on the surface of Fe_3O_4 nanoparticles matrix. The bands observed at 1710 cm^{-1} and 1642 cm^{-1} in Fig. 1c could be attributed to the stretching frequency of C=O and C=C respectively (amide 1 band).

The L-Histidine-Fe_3O_4 absorption bands at 3411 cm^{-1} corresponding to the stretching vibration of O–H were recorded together with the N–H absorption bands. The absorption bands in the range of 3030-3130 cm^{-1} are due to asymmetric valence vibrations of the ammonium (NH_3^{+}) group. The symmetric absorption vibrations in 2080-2140 cm^{-1} or 2530-2760 cm^{-1}, depend on amino acid chemical structures. The peak of bending absorption of carboxylate (COO^-)

View Article Online
DOI: 10.1039/C6RA19776K

group appears at 1610-1641 cm^{-1}. The bands appeared at 1144 and 1622 cm^{-1} can be assigned to the vibration of C-N and C=N in imidazolium rings, respectively.

The infrared spectrum of the Cu(II)/L-His@Fe_3O_4 complex has shown changes in the position and profiles of some bands as compared to those of the free L-Histidine@Fe_3O_4, suggesting participation of the groups that produce these bands in the coordination with copper atoms. Major changes are related to the carboxylate and amine bands. The infrared spectrum of the Cu(II)/L-His@Fe_3O_4 complex exhibits (Cu-O) and (Cu -N) stretching bands at 973 cm^{-1} and 448 cm^{-1}, respectively. These results confirm the introduction of carboxylate and amino nitrogen groups of L-Histidine to Cu (II) ions through coordination mode.

The infrared spectrum of recovered catalyst (Fig. 1f) indicates that the catalyst can be recycled six times without any significant change in its structure.

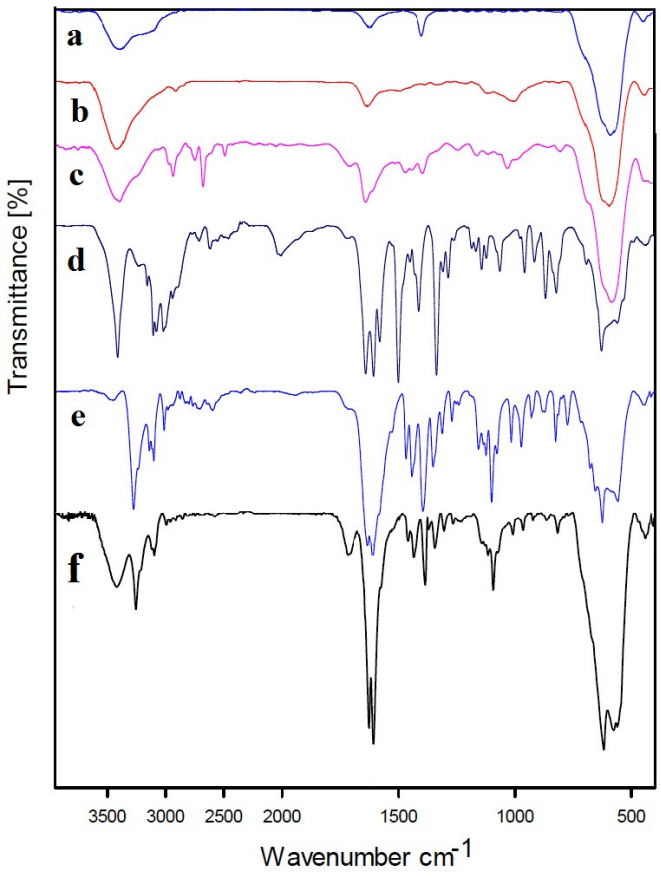

Fig. 1. FT-IR spectra of (a) Fe_3O_4 nanoparticles, (b) amino-functionalized (c) MNP-acryloxyl, (d) L-His@Fe_3O_4, (e) Cu(II)/L-His@Fe_3O_4 and (f) recovered catalyst

TGA/DTA analysis of the samples is presented in Fig. 2. We assign the first weight loss to water leaving the sample. The latter losses are assigned to decomposition of iron oxide phase transitions to thermodynamically more stable Fe_2O_3 phase (the DTA patterns are the signature of the recrystallization and phase transformation from Fe_3O_4 to γ-Fe_2O_3).

The TGA curve of Cu(II)/L-His@Fe_3O_4 showed the first weight loss below 100 °C due to desorption of physisorbed water. This was followed by a gradual decrease in the weight after 250 °C. The metal-organic structure grafting to the Fe_3O_4 surface were decomposed in the temperature range of 250 to 450°C. The exothermic peak at about 402°C indicated the beginning of decomposition of the organic surfactant, the amount of loading organic groups is estimated to be 26.87% (*w*/*w*).

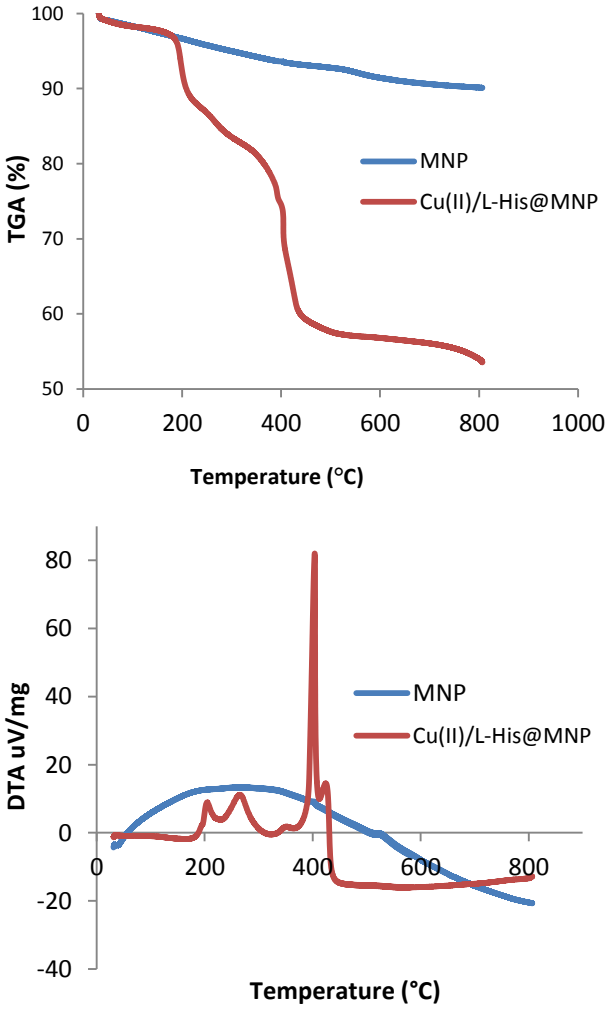

Fig. 2. TGA/DTA curves of Fe_3O_4 and Cu(II)/L-His@Fe_3O_4.

Fig. 3 shows the magnetic curve for Fe_3O_4 nanoparticles and Cu(II)/L-His@Fe_3O_4 catalyst. Ms value for Cu(II)/L-His@Fe_3O_4 nanoparticle was found to be 34.7 $emug^{-1}$, which is lower than the saturation magnetization of the Fe_3O_4 bulk materials (77 $emug^{-1}$). This decrease in Ms could mainly be attributed to the small particle

surface effect that becomes more prominent as the particle size decreases.

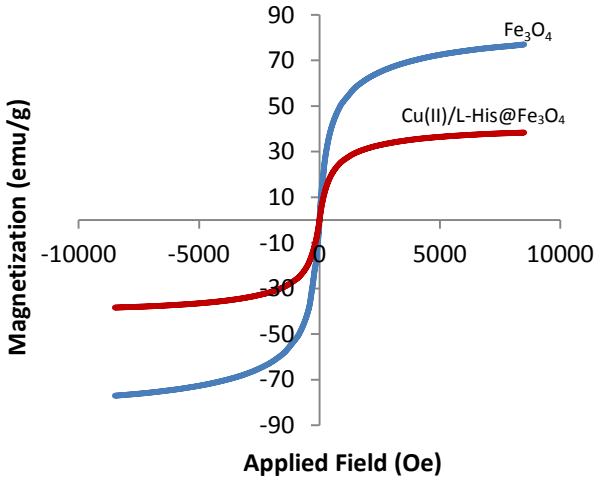

Fig. 3. Magnetization curves for Fe_3O_4 and Cu(II)/L-His@Fe_3O_4

SEM images of Cu (II)/L-His@Fe_3O_4 at different magnification (a-b) and EDS pattern of Cu (II)/L-His@Fe_3O_4(c) are shown in Fig. 4.

The Scanning electron microscopy (SEM) of Cu(II)/L-His@Fe_3O_4 materials shows that they consist of spherical particles and have a relatively uniform diameter of 8-15 nm (Fig. 4a-b). The shape of the support is retained after immobilization of the metal complexes. The electron dispersive spectroscopy (EDS) spectra of the Cu(II)/L-His@Fe_3O_4 was taken at random points on the surface.

The EDS results of the core–shell structure confirms the presence of Si, C, O, N, Fe, and Cu elements, indicating the successful attachment of the Copper(II)–L-Histidine on the surface Fe_3O_4 MNPs (Fig. 4c).

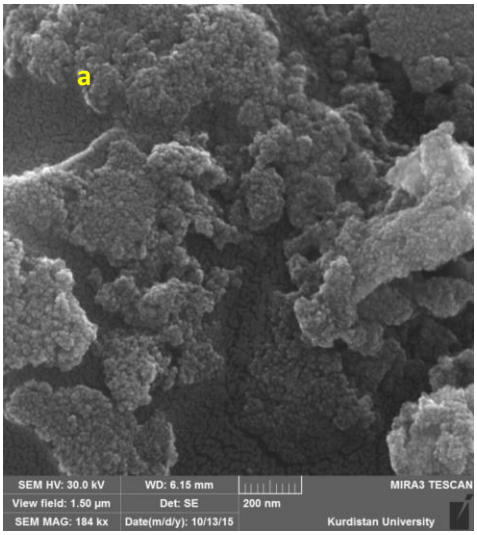

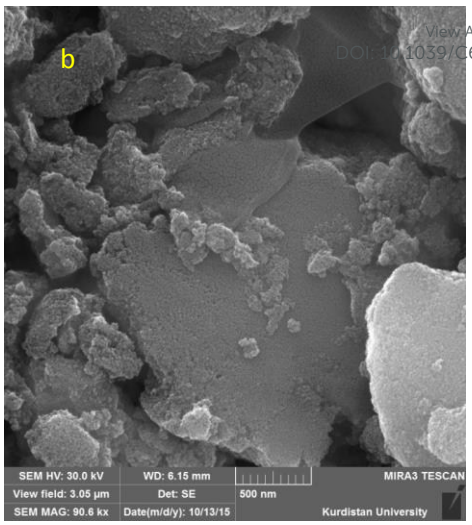

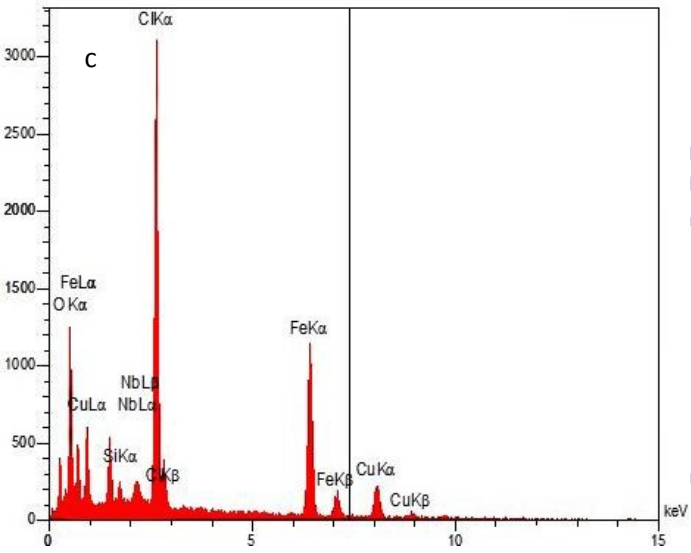

Fig.4. SEM images of Cu(II)/L-His@Fe_3O_4 at different magnification (a-b). EDS pattern of Cu(II)/L-His@Fe_3O_4 (c).

Powder XRD diffraction patterns (Fig. 5) obtained for the Copper(II)–L-Histidine exhibited very broad peaks indicating the ultrafine nature and small crystallite size of the particles. The diffraction peaks located at 20.94°, 35.25°, 41.48°, 50.72°, 63.02°, 67.50°, and 74.72° have been keenly indexed as a cubic spinel structure. The average particle size of the sample was found to be 14.28 nm which is derived from the FWHM of more intense peak corresponding to 311 planes located at 41.48° using Scherrer's formula.

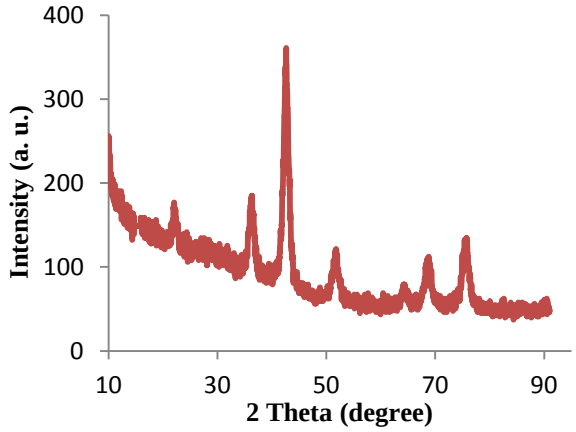

Fig. 5. XRD patterns of Cu(II)/L-His@Fe_3O_4.

The Cu loading of the prepared catalyst, measured by coupled plasma (ICP-AES) analysis, showed a value of about 0.96 mmol/g of catalyst.

ICP-AES analysis of catalysts recycled showed minor changes of Cu contents (0.92 mmol/g). These phenomena indicate that the multi component reactions indeed go through a heterogeneous catalytic reaction process. In addition, the very low metal leached during the reaction.

The transmission electron microscopy (TEM) image of Cu (II)/L-His@Fe_3O_4 and recovered catalyst are illustrated in Fig. 6a and b. Particles are observed to have spherical morphology from Fig. 6a and b. Average particle size is estimated at 5-15 nm which show a close agreement with the values calculated by XRD analysis. TEM image of recycled catalyst was showed that the morphology of Cu(II)/L-His@Fe_3O_4 remained after recovery (Fig. 6b).

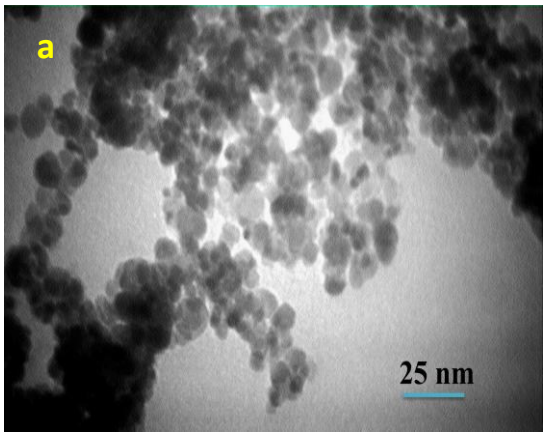

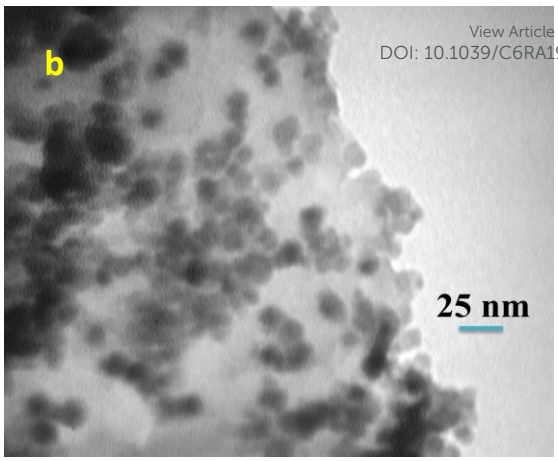

Fig.6. TEM images of (a) Cu (II)/L-His@Fe_3O_4 and (b) recovered catalyst.

Catalytic studies

In continuation of our interest on environmentally benign chemical processes for synthesis of biologically molecules [30–35], we developed a new method for preparation of a stable, cheap and efficient heterogeneous Cu(II)/L-His@Fe_3O_4 nanocatalyst which has been used with excellent activity in multi component reactions (Scheme 4 and 5).

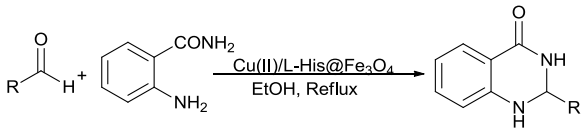

Scheme 4. Synthesis of 2,3-dihydroquinazolin-4(1H)-ones.

In the first part of our program, the catalytic activity of Cu(II)/L-His@Fe_3O_4 was evaluated in the synthesis of 2,3-dihydroquinazolin-4(1H)-ones (DHQ) derivatives. In order to optimize the reaction conditions, the reaction of 4-chlorobenzaldehyde with 2-aminobenzamide was chosen as a model reaction. As shown in Table 1, different amounts of catalyst between 2-6 mg were used for this reaction, and 4 mg of Cu(II)/L-His@Fe_3O_4 nanocatalyst was found to be optimal. For higher amounts of the catalyst, the desired product was obtained in a nearly quantitative yield (Table 1, entries 5).

In the second part of our investigation, we demonstrated that Cu(II)/L-His@Fe_3O_4 can also be used in the synthesis of polyhydroquinolines (PHQ) derivatives (Scheme 5).

View Article Online
DOI: 10.1039/C6RA19776K

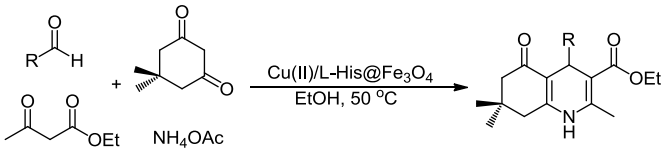

Scheme 5. Synthesis of polyhydroquinolines.

During our initial studies, 4-chlorobenzaldehyde was selected as substrates for the model reaction. Various conditions were screened and the results are summarized in Table 1.

The reactions was carried out in the absence and presence of Cu(II)/L-His@Fe_3O_4 catalyst. It was found that in the absence of the catalyst the reaction was slightly sluggish and only trace amount of product was obtained after 24 h. But when the reaction was conducted in the presence of Cu(II)/L-His@Fe_3O_4 (4 mg), the reaction was completed yielding (98%) in 120 min (entry 4).

Finally, the outset, the model reaction was carried out in the presence of 4 mg catalyst in ethanol at 50 °C temperature.

Table 1: Optimization of the amount of the Cu(II)/L-His@Fe_3O_4

Entry	Catalyst (mg)	Yield of DHQ[a] (%)	Yield of PHQ[b] (%)
1	-	Trace[c]	32
2	2	55	62
3	3	70	80
4	4	99	98
5	6	99	98

[a] Reaction conditions for the synthesis DHQ: 4-chlorobenzaldehyde (1 mmol), 2 aminobenzamide (1 mmol) and ethanol solvent (10 mL) at reflux temperature.

[b]Reaction conditions for the synthesis PHQ: 4-chlorobenzaldehyde (1 mmol), dimedone (1 mmol) , ethyl acetoacetate (1 mmol), ammonium acetate (1.2 mmol).

Under the optimized reaction conditions, the generality of substrates was checked next. Different aldehydes were used for the synthesis of 2, 3-dihydroquinazolin-4(1H)-ones (Table 2) and polyhydroquinolines derivatives (Table 3). As shown in Table 2 and 3 most of the aromatic and aliphatic aldehydes would give the prouducts in good yields. A variety of functional groups of aldehydes are known to tolerate this reaction condition, which include alkoxyl, methyl, nitro, Cl, F, and OH groups. However, the substituents on the phenyl ring of aromatic aldehydes had same influence on the yields.

Table 2

Synthesis of 2,3-dihydroquinazolin-4(1H)-one derivatives

Entry	Aldehyde	Product	Time (min)	Yield[b] (%)	Mp (°C) [Ref.]
1	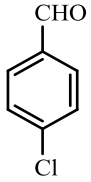	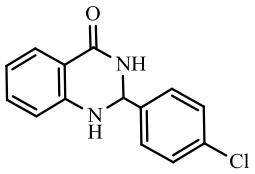	25	99	202-203[30]
2	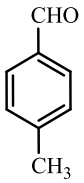	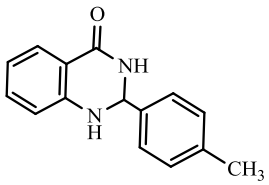	10	98	225-226[30]
3	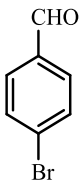	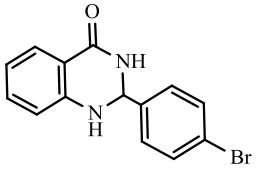	40	97	197-200[30]

View Article Online
DOI: 10.1039/C6RA19776K

4	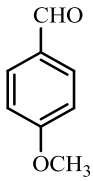	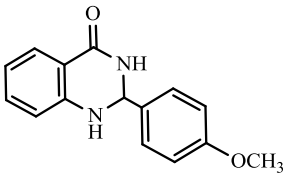	10	98	182-183[30]
5	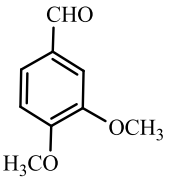	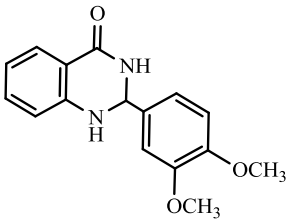	23	94	211-212[30]
6	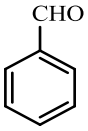	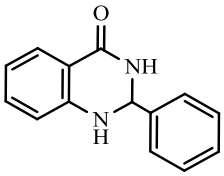	15	96	223-224[30]
7	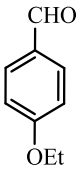	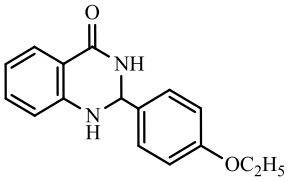	35	98	167-168[30]
8	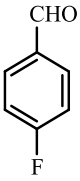	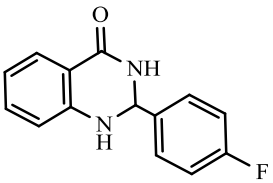	25	98	192-193[30]
9	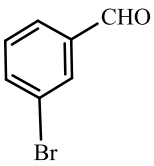	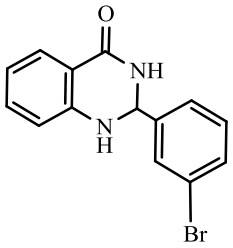	32	96	184-185[30]
10	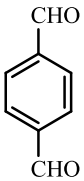	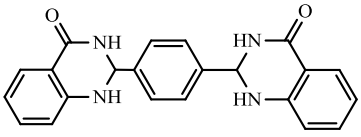	60	94	244-245[30]
11	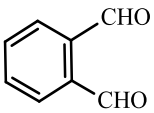	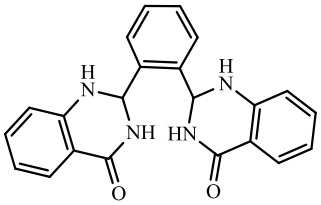	80	86	272-273[30]

View Article Online
DOI: 10.1039/C6RA19776K

12	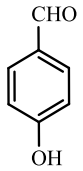	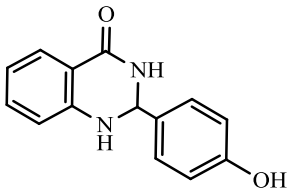	23	98	280-282[21]
13	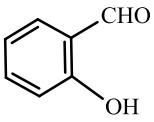	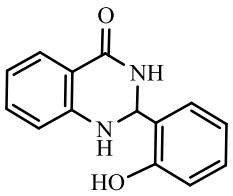	15	98	220-222[21]
14	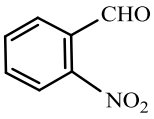	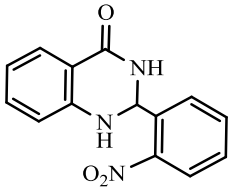	50	96	191–192[21]
15	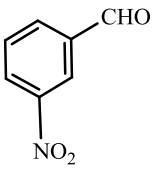	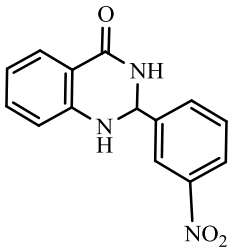	100	84	202–204[21]
16	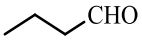	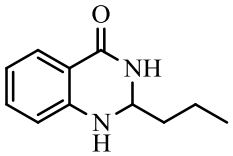	17	98	157-159[30]
17	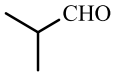	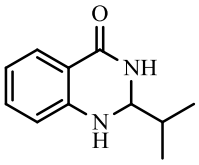	45	96	160-164[31]

[a] Reaction conditions: aldehyde (1 mmol), 2-aminobenzamide (1 mmol), catalyst (4 m g) and ethanol solvent (5mL) at reflux temperature.

[b] Isolated yields

Table 3

Synthesis of polyhydroquinolines derivatnives

Entry	Aldehyde	Product	Time (min)	Yield[b] (%)	Mp (°C) [Ref.]

View Article Online
DOI: 10.1039/C6RA19776K

1	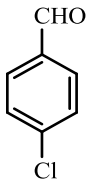	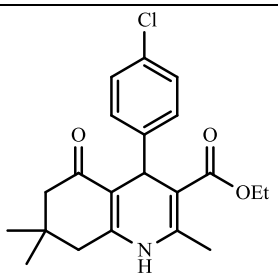	90	98	239-241[17]
2	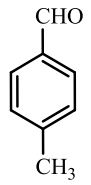	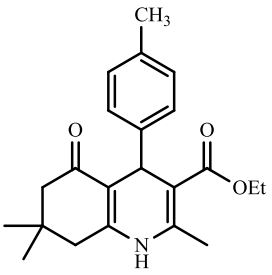	120	96	252-254[17]
3	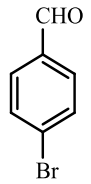	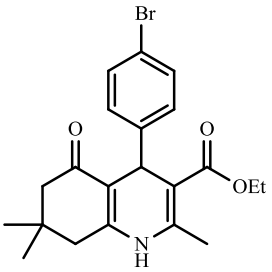	110	96	249-252[32]
4	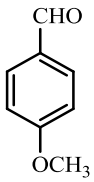	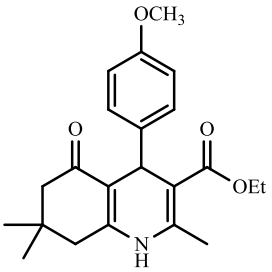	100	94	247-249[17]
5	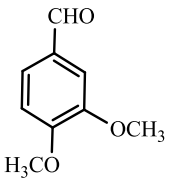	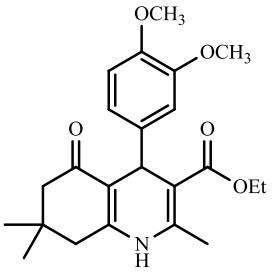	90	95	201-202[17]
6	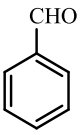	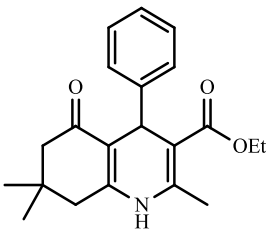	95	92	207-209[17]

View Article Online
DOI: 10.1039/C6RA19776K

7	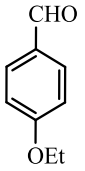	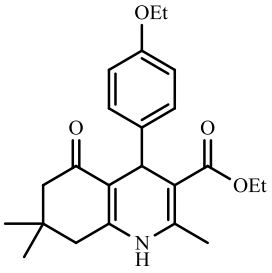	110	98	176-178[32]
8	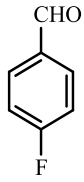	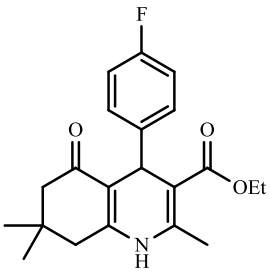	100	90	183-185[17]
9	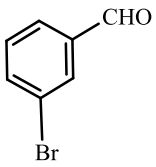	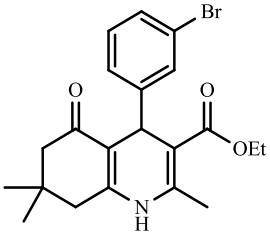	90	96	234-236[19]
11	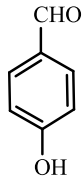	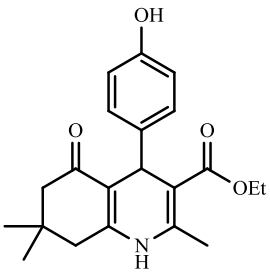	90	96	230-232[17]
11	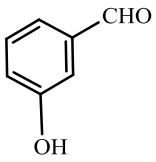	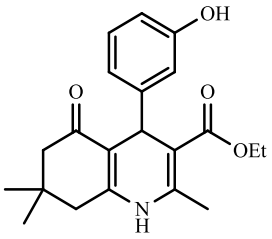	100	93	217-219[17]
12	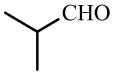	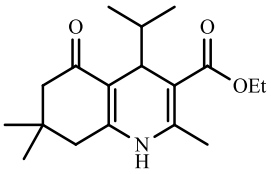	150	92	162-164[17]
13	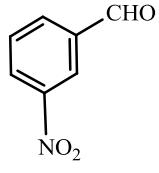	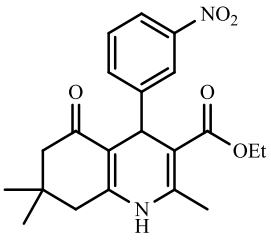	120	92	170-172[17]

View Article Online
DOI: 10.1039/C6RA19776K

14	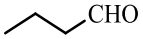	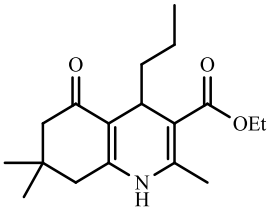	90	91	146-147[17]

[a] Reaction conditions: arylaldehyde (1mmol), dimedone (1 mmol),ethyl acetoacetate (1 mmol), NH_4OAc (1.2 mmol), catalyst (4 m g) and ethanol solvent (5mL) at 50 °C.

[b] Isolated yields

During the course of one of our drug discovery programs, we became interested in the synthesis of 2-amino-6-(arylthio) pyridine-3,5-dicarbonitrile (Scheme 6). These pyridine derivatives are a privileged scaffold for developing pharmaceutical agents because various compounds with this structural motif display significant and diverse biological activities.

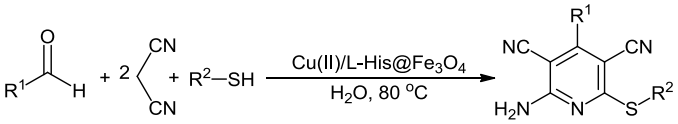

Scheme 6. Synthesis of 2-amino-6-(arylthio) pyridine-3,5-dicarbonitrile.

We initiated our study with the reaction between 4-methoxybenzaldehyde, 4-bromobenzenethiol and malononitrile as a model reaction (Table 4).

Subsequently, we agreeably found out that the presence of 5 mg of Cu(II)/L-His@Fe_3O_4, promoted the reaction efficiently and improved the yield to 91% (entry 4). The nature of solvent was then screened. In water, the reaction also proceeded smoothly and gave a good yield. In acetonitrile, however, only a low yield of (30%) was obtained (entry 6). When the reaction was carried out in, ethanol, almost no desired product was found (entries 7). Based on the above mentioned reasons, it was found that the water is the best solvent. The effect of temperature on reaction was examined.With increasing the temperature the yield of product also increases and It was found that optimal reaction temperature is 80 °C

Table 4

Optimization of reaction conditions for the one-pot synthesis of pyridines

Entry	Solvent	Catalyst (mg)	Time (min)	Yield[b] (%)
1	H_2O	No catalyst	24h	Treac
2	H_2O	2	60	23
3	H_2O	3	60	61
4	H_2O	5	60	91
5	H_2O	7	60	90
6	Acetonitrile	5	60	30
7	EtOH	5	60	trace

[b]Reaction conditions: 4-methoxybenzaldehyde (1 mmol), 4-bromobenzenethiol (1 mmol), malononitrile (2 mmol) in water (5 mL) at 80 °C for 60 min.

With the optimal reaction conditions in hand (Table 4, entry 4), the scope and generality of this protocol was investigated next. A wide variety of aromatic aldehydes and thiols were used for synthesis of 2-amino-3,5-dicarbonitrile-6-thio-pyridines. The results are summarized in Table 5. Meanwhile, the electronic properties and different positions of the substituents have no obvious effect on the reaction yields.

Table 5 Synthesis of 2-amino-3,5-dicarbonitrile-6-thio-pyridines[a]

Entry	Aldehyde	Thiophenol	Product	Yield[b] (%)	Mp (°C) [Ref.]

View Article Online
DOI: 10.1039/C6RA19776K

1	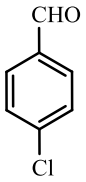	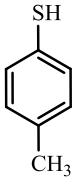	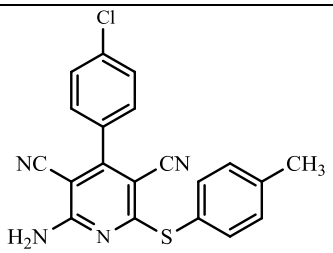	92	238-240[29]
2	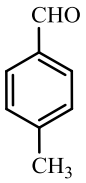	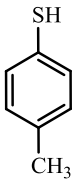	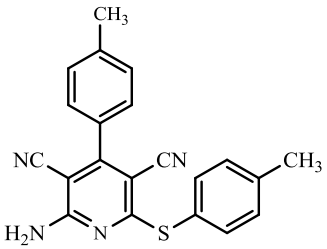	90	220-222[28]
3	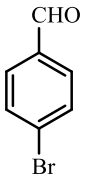	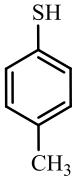	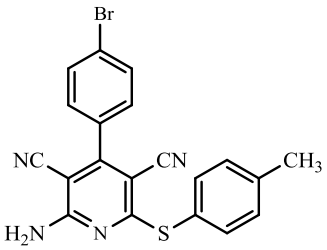	86	238-239[25]
4	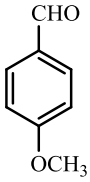	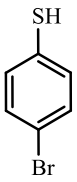	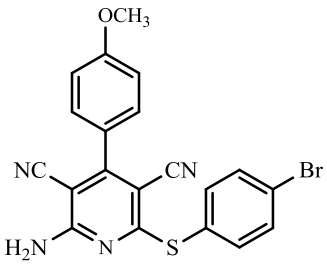	91	233-235[26]
5	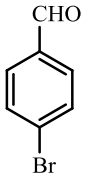	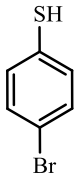	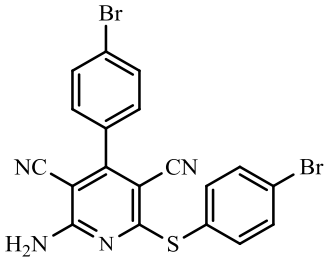	89	230-232[26]
6	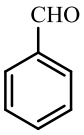	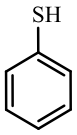	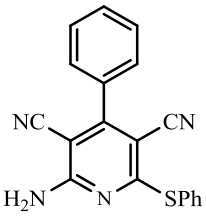	95	217-218[27]

View Article Online
DOI: 10.1039/C6RA19776K

7	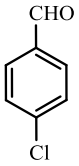	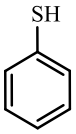	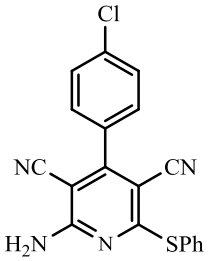	94	221-223[27]
8	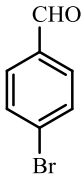	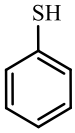	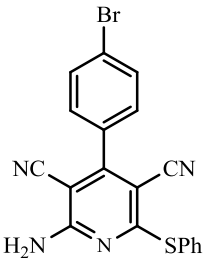	87	245-250[26]
9	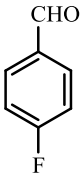	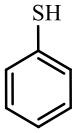	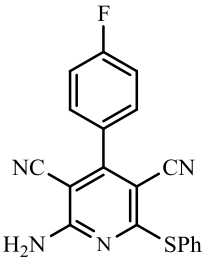	97	223-225[27]
11	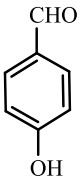	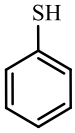	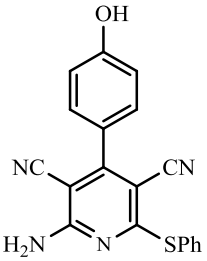	94	315-317[27]
11	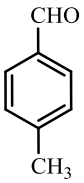	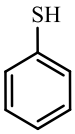	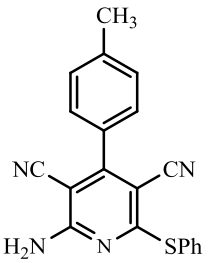	92	211-212[27]
12	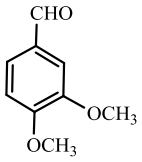	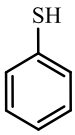	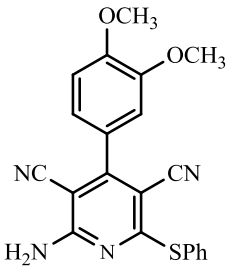	89	225-227[27]

View Article Online
DOI: 10.1039/C6RA19776K

[a]

13	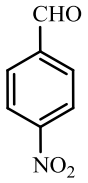	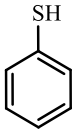	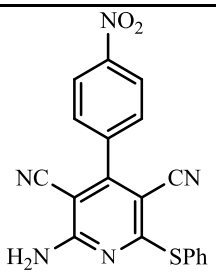	90	288-290[27]
14	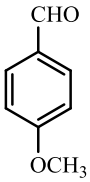	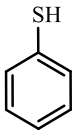	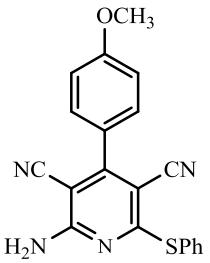	93	240-242[27]

Reaction conditions: arylaldehyde (1mmol), thiol (1 mmol), malononitrile (2 mmol), catalyst (5 mg) and in water (5 mL) at 80 °C for 60 min.

[b] Isolated yields.

Based on industrial green chemistry principles, the reusability of the catalyst is important for the large scale operation. Therefore, reusability of described catalyst was examined for the synthesis DHQ (Table 2, entry 1) and PHQ (Table 3, entry 1). After the first run, the catalyst was easily and rapidly separated from the reaction mixture using an external magnet and subsequently was used for the next run. As it can be seen from Fig. 7, the catalyst can be recycled at lease for six runs without any significant loss of its catalytic activity and efficient.

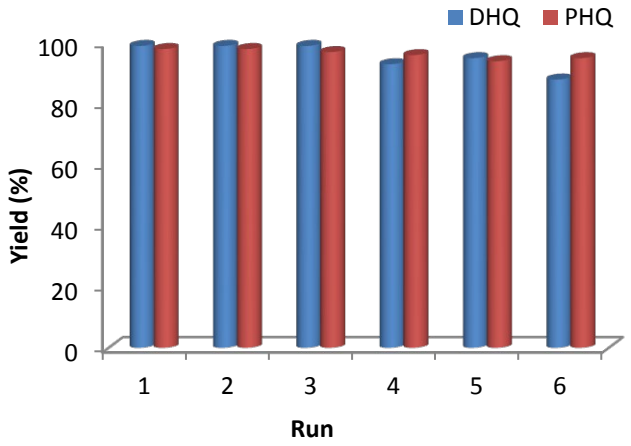

Fig. 7. Recycling of Cu(II)/L-His@Fe_3O_4 for the model reaction under optimized conditions

In summary, we have successfully developed an efficient and novel catalyst for several synthetic organic transformations. Cu(II)-L-Histidine was grafted onto magnetic Fe_3O_4 nanoparticles, as a metal-chelating monomer via metal coordination interactions and histidine template. Copper (II) bound to L-histidine is in equilibrium with human serum albumin and may undergo mutual exchange which modulates the bioavailability of copper to the cell. A range of corresponding products were synthesized by this strategy with moderate to good yields under mild and green conditions in a heterogeneous system with short reaction times. These nanocatalysts have emerged as powerful tools for the efficient conversion of raw materials into useful chemicals of both industrial and pharmaceutical significance.

Furthermore, the Cu(II)/L-His@Fe_3O_4 nanocatalyst can be easily separated from the reaction mixture and the catalytic activity remained unchanged even after 6 successive recycling experiments.

Experimental

Materials

All the reagents and solvents were purchased from Sigma-Aldrich, Fluka or Merck and utilized without further purification.

The particle morphology was examined by measuring SEM using FESEM-TESCAN MIRA3. The products component measurement was carried out by the energy dispersive spectroscopy (EDS) using FESEM-TESCAN MIRA3 scanning electron microscopes. The thermogravimetric analysis (TGA) curves are recorded using a Shimadzu DTG-60 instrument. VSM measurements were performed using a Vibrating Sample Magnetometer (VSM) MDKFD. The magnetization measurements were carried out in an external field up to 15 kOe at several temperatures.

View Article Online
DOI: 10.1039/C6RA19776K

Nanostructures were characterized using a Holland Philips X'pert X-ray powder diffraction (XRD) diffractometer (Co Ka, radiation= 0.154056 nm). IR spectra were recorded as KBr pellets on a VRTEX 70 model BRUKER FTIR spectrophotometer. NMR spectra were recorded on a Bruker Avance III 400MHz. Chemical shifts are given in ppm (δ) relative to internal TMS and coupling constants *J* are reported in Hz. Melting points were measured with an Electrothermal 9100 apparatus. The Cu amount of catalyst was measure by Inductively Coupled Plasma Atomic Emission Spectrometer (ICP-OES). The particle size and morphology were investigated by a Zeiss-EM10C transmission electron microscope (TEM) on an accelerating voltage of 80 kV.

Preparation of Cu(II)/L-His@Fe_3O_4 catalyst

Acryloyl chloride-coated magnetic nanoparticles (MNP-acryloxyl) were prepared according to the literature method [29]. The resulting materials were dispersed in ethanol (10.0 mL), and then L-Histidine (3.2 mmol) was added to it and stirred continuously for 1 week at room temperature. The L-His@Fe_3O_4 particleswere separated by a magnetic field, washed with ethanol and dried under vacuum for 12 h.

The L-His@Fe_3O_4 (0.5 g), was added to the round-bottom flask containing a solution of Copper (II) chloride (0.25 g) in ethanol (20 mL). The mixture was then stirred vigorously under reflux conditions for 8 h. The solid was separated by magnetic decantation. The magnetic catalyst was washed with copious amounts of ethanol and dried under vacuum at room temperature.

General synthesis for the preparation of 2,3-dihydroquinazolin-4(1H)-ones

A mixture of aldehyde (1 mmol), 2-aminobenzamide (1mmol), Cu(II)/L-His@Fe_3O_4 (4 mg) and ethanol (4 mL) was stirred at 80 °C. Upon completion, the progress of the reaction was monitored by TLC. After the TLC indicates the disappearance of starting materials, the reaction was cooled to room temperature. The catalyst was separated by an external magnet and reused as such for the next experiment. The filtrate was evaporated to remove solvent, the resultant solid was then washed with ethanol to obtain pure 2,3-dihydroquinazolin-4(1H)-ones in 89-99% yields.

2-(4-chlorophenyl)-2,3-dihydroquinazolin-4(1H)-one (Table 2, entry 1)**:** White solid, Mp: 202-203 °C. ^{1}H NMR (250 MHz, DMSO-d_6): δ 8.29 (s, 1H), 7.61-7.41 (m, 5H), 7.26-7.2 (t, 1H), 6.75-6.63 (m, 2H), 7.12 (s, 1H), 6.75-6.63 (m, 2H), 5.75 (s, 1H) ppm. ^{13}C NMR (62 MHz, DMSO-d_6): δ 163.9, 148.1, 141.1, 133.8, 133.4, 129.2, 128.7, 127.8, 117.7, 115.4, 114.9, 66.2 ppm.

2-(4-methylphenyl)-2,3-dihydroquinazolin-4(1H)-one (Table 2, entry 2)**:** White solid, Mp: 225-226 °C. ^{1}H NMR (250 MHz, DMSO-*d*6): δ 8.21 (s, 1H), 7.62-7.59 (d, 1H), 7.38-7.35 (d, 2H), 7.26-7.16 (m, 3H), 7.03 (s, 1H), 6.75-6.63 (m, 2H), 5.71 (s, 1H), 2.49-2.42 (s, 3H) ppm.^{13}C NMR (62 MHz, DMSO-*d*6): δ 164.1, 148.4, 139.1, 138.2, 133.7, 129.3, 127.8, 127.2, 117.5, 115.4, 114.9, 66.8, 21.2 ppm.

2-(4-ethoxyphenyl)-2,3-dihydroquinazolin-4(1H)-one (Table 2, entry 7): White solid, m.p. 167–168 °C, ^{1}H NMR (400 MHz, $CDCl_3$): δ (ppm) 7.98 (brs, 1H), 7.6 (d, J = 6 Hz, 2H) 7.34 (s, 1H), 7.26 (d, J = 2 Hz, 1H), 6.87–7.03 (m, 3H), 6.65 (d, J = 5.6 Hz, 1H), 5.87 (s, 1H), 5.75 (s, 1H), 4.12 (t, J= 4 Hz, 2H) 1.45 (q, J= 6.4 Hz, 3H). ^{13}C NMR (100MHz, $CDCl_3$): δ 161.4, 148.9, 147.5, 131.52, 129.89, 120.7, 116.79, 116.01, 115.68, 69.82, 64.78, 15.9; IR (KBr): mmax 3300, 3060, 3000, 2930, 1666, 1650, 1610, 1487, 1387, 70.

2,2'-(1,2-phenylene)bis(2,3-dihydroquinazolin-4(1H)-one) (Table 2, entry 11): White solid, m.p. 272-273 °C, ^{1}H NMR (400 MHz, DMSO): δ (ppm) 7.87 (d, J = 8.4 Hz, 4H), 7.64 (s, 2H), 7.46 (s, 2H), 7.32 (d, J = 6 Hz, 2H), 7.15 (s, 2H), 6.69 (s, 3H), 6.63 (s, 2H), 5.75 (s, 2H). IR (KBr): mmax 3299, 3248, 3181, 2961, 2831, 1698, 1639, 1808, 1515, 1481, 1297, 1151, 742.

2-isopropyl-2,3-dihydroquinazolin-4(1H)-one (Table 2, entry 17): White solid, m.p. 160–164°C,^{1}H NMR (400 MHz, $CDCl_3$): δ = 7.88 (d, J = 7.6 Hz, 1H), 7.31 (t, J = 7.2 Hz, 1H), 6.84 (t, J = 7.2 Hz, 1H), 6.74 (s,1), 6.69 (d, J = 8 Hz, 1H), 4.72 (d, J= 4.4, 1H), 2.00 (m, 6H), 1.05 (d, J = 6.8 Hz, 6H). ^{13}C NMR (100 MHz,CDCl3): δ =, 165.52, 147.55, 133.87, 128.46, 118.97, 115.52, 114.51, 70.16, 32.82, 148.9, 16.94.

General method for the synthesis of polyhydroquinolines

4 mg of Cu(II)/L-His@Fe_3O_4 catalyst was ultrasonically dispersed in freshly distilled ethanol (5 mL). Then, a mixture of aldehydes (1 mmol), dimedone (1 mmol), ethyl acetoacetate (1 mmol) and ammonium acetate (1.2 mmol) was added. The resulting mixture was stirred at 50°C for the appropriate time, as shown in Table 3. After completion of the reaction the catalyst was separated from the reaction mixture using an external magnet. Subsequently, the solvent was evaporated and the residue was purified by further recrystallisation in ethanol. A wide range of products were obtained in good to excellent yields (91−98%).

View Article Online
DOI: 10.1039/C6RA19776K

Ethyl 2,7,7-trimethyl-5-oxo-4-(p-tolyl)-1,4,5,6,7,8-hexahydroquinoline-3-carboxylate (Table 2, entry 3)**:**White solid, M.p. 252-254°C, ^{1}H NMR (400 MHz, CDCl3) δ: 9.05 (s, 1H, NH), 7.01-7.29 (m, 4H), 5.03 (s, 1H), 4.04 (q, j= 8.2HZ, 2H), 2.21 (m,3H), 2.28 (s, 3H), 1.96 (s, 1H), 1.25 (t, J =7.2 Hz, 3H), 1.11 (s, 3H), 0.98 (s, 3H) ppm. IR (KBr, cm^{-1}): 3274, 2956, 1699, 1603, 1488, 1378, 1233, 1139, 1030, 748, 743.

Ethyl 4-(3,4-dimethoxyphenyl)-2,7,7-trimethyl-5-oxo-1,4,5,6,7,8-hexahydroquinoline-3-carboxylate (Table 3, entry 5)**:** White solid, M.p. 201-202°C, IR (kbr, cm^{-1}): 3203, 2958, 1692, 1601, 1485, 1378, 1216, 1139, 1029, 758, 730. 1H NMR (400 mhz, DMSO-d6) δ: 9.06 (s, NH) 6.74 (d, J=16 H, 2H), 6.65 (d, J =8 Hz, 1H), 4.80 (s, 1H), 4.02 (d, J=8 Hz, 2H), 3.67 (s, 6H), 2.42 (d, J=8 Hz, 1H), 2.28-2.32 (m, 4H), 2.21 (d, J=16 Hz, 1H), 2.02 (d, J=14 Hz, 1H), 1.17 (s, 3H), 1.03 (s, 3H), 0.90 (s, 3H) ppm. ^{13}CNMR (100 mhz, DMSO-d6) δ: 194.8, 161.4, 149.9, 148.3, 147.4, 145.1, 144.9, 140.9, 119.6, 112.1, 111.9, 110.5, 104.3, 59.5, 55.8, 50.7, 35.6, 32.6, 29.7, 26.9, 18.7, 18.6, 14.7 ppm.

Ethyl 4-(4-ethoxyphenyl)-2,7,7-trimethyl-5-oxo-1,4,5,6,7,8-hexahydroquinoline-3-carboxylate (Table 2, entry 7)**:** White solid, M.p. 176-178 °C, ^{1}H NMR (400 MHz, CDCl3): δ= 7.19 (d, J = 6.4 Hz, 2H) , 6.73 (d, J = 6.4 Hz, 2H), 5.80 (s, 1H), 4.99 (s, 1H), 4.06 (t, 2H), 3.96 (t, 2H), 2.15-2.38 (m, 7H), 1.37-1.38 (m, 3H), 1.20-1.21 (m, 3H), 1.07 (s, 3H), 0.95 (s, 3H) ppm. ^{13}C NMR (100 MHz, CDCl3): δ= 198, 169, 158.3, 150.2, 144.7, 140.7, 130.1, 114.9, 113.1107.3, 64.3, 60.9, 51.9, 41.8, 36.8, 33.7, 30.6, 28.2, 20.3, 16.05, 15.4 ppm.

Ethyl 4-(3-hydroxyphenyl)-2,7,7-trimethyl-5-oxo-1,4,5,6,7,8-hexahydroquinoline-3-carboxylate (Table 2, entry 11): White solid, M.p. 217-219°C, IR (KBr, cm^{-1}): 3274, 2950, 1690, 1600, 1497, 1377, 1214, 1144, 1033, 782, 722. ^{1}H NMR (400 MHz, DMSO-d6) δ: , 9.10 (s, OH), 9.04 (s, NH), 6.46-6.98 (m,4H) , 4.80 (s, 1H), 3.98 (q, J=4 Hz, 2H), 2.44 (d, J = 16 Hz, 1H), 2.28 (q, J=12 Hz, 3H), 2.17 (d, J=16 Hz, 1H) , 2.00 (d, J=16 Hz, 1H), 1.61 (t, J =7.2 Hz, 3H) , 1.02 (s, 3H), 0.88 (s, 3H).^{13}C NMR (100 MHz, DMSO-d6) δ: , 193.9, 166.0, 194.7, 167.4, 157.3, 149.9, 149.4, 145.2, 129.0, 118.6, 115.0, 113.0, 110.2, 104.1, 59.5, 55.7, 50.7, 36.0, 32.6, 29.6, 27.0, 18.06, 18.7, 14.6.

General method for synthesis of 2-amino-3,5-dicarbonitrile-6-thio-pyridines

To a stirred solution of aldehyde (1 mmol), malononitrile (2 mmol) and thiols (1 mmol) in water (4 mL), Cu(II)/L-His@Fe_3O_4 (5 mg) was added and the reaction mixture was stirred at 80 °C for 60 min. After reaction completion, the catalyst was separated by an external magnet and reused as such for the next experiment. The mixture was diluted with ethyl acetate and water solution and the extracted organic layer was dried over Na_2SO_4 (1.5 g) and the solvent was evaporated. The crude product was recrystallized from ethanol to obtain pure product.

2-amino-4-(4-fluorophenyl)-6-(phenylthio)pyridine-3,5 dicarbonitrile (Table 5, entry 9): Yellow solid, Mp 223-225°C, ^{1}H NMR (300 MHz, DMSO-d6) δ: 7.81 (d, *J* = 8.1 Hz, 2H), 7.60–7.59 (m, 2H), 7.55–7.51 (m, 5H), 5.51 (s, 2H).

2-Amino-4-(4-methoxy-phenyl)-6-phenylsulfanyl-pyridine-3,5-dicarbonitrile (Table 5, entry 14)**:** Yellow solid, Mp 240-242°C, ^{1}H NMR (300 MHz, $CDCl_3$) δ: 7.43–7.59 (m, 7H), 7.08 (d, *J* = 8.8 Hz, 2H), 5.46 (s, 2H), 3.91 (3H, s).

Complete experimental procedures and relevant spectra (^{1}H NMR and ^{13}C NMR) for several prepared compounds, and the catalyst characterization data are available in the Supporting information.

Acknowledgements

Authors thank Ilam University for financial support of this research project.

References

1 V. Feyer, O. Plekan, S. Ptasińska, M. Iakhnenko, N. Tsud, K.C. Prince J. *Phys. Chem. C.* 2012, **116**, 22960.

2 D. J. Sullivan, I. Y. Gluzman, D. E. Goldberg, *Science* 1996, **271**, 219.

3 A. L. Jones, M. D. Hulett, Parish, C. R. *Immunol. Cell Biol.* 2005, **83**, 106.

4 G. N. Chen, X. P. Wu, J. P. Duan, H. Q. Chen, *Talanta* 1999, **49**, 319.

5 Y. Hu, Q. Wang, C. Zheng, L. Wu, X. Hou, Y. Lv, *Anal. Chem.* 2014, **86**, 842.

6 F. Carrera, E. S. Marcos, P. J. Merkling, J. Chaboy, A. Munoz-Paez, *Inorganic Chemistry*, 2004, **43**, 6674.

7 S. J. Lippard, J. M. Berg, *University Science Books: Mill Valley, CA, USA,* 1994.

8 P. Deschamps, P. P. Kilkarni, M. Gautam-Basak, B. Sarkar, *Coord. Chem. Rev.* 2005, **249**, 895.

9 L. Gala, M. Lawson, K. Jomova, L. Zelenicky, A, Congradyova, M. Mazur, M. Valko, *Molecules*, 2014, **19**, 980.

10 B. Sarkar, T. P. A. Kruck, J. Peisach, P. Aisen, W. Blumberg (Eds.), *Biochemistry of Copper, Academic Press, New York*, 1966, p. 183.

11 B. Sarkar, *Chem. Rev.* 1999, **99**, 2535.

12 B. Evertsson, Acta Cryst. 25 (1969) 30–41.

13 M. Kooti, M. Afshar, *Mater. Res. Bull.* 2012, **47**, 3473.

14 M. Sheykhan, L. Ma'mani, A. Ebrahimi, A. Heydari, *J. Mol. Catal. A Chemical.* 2011, **335**, 245.

15 B. Panella, A. Vargas, A. Baiker, *J. Catal.* 2009, **261**, 88.

16 S. Venkateswarlu, M. Satyanarayana, K. Srinivas, Kodumuri N. V. V. Aadisudhakar, *Tetrahedron Lett.* 2013, **54**, 128.

17 M. Tajbakhsh, H. Alinezhad, M. Norouzi, S. Baghery, M. Akbari. *J. Mol. Liquid.* 2013, **177**, 44.

18 M. Abdollahi-Alibeik, A. Rezaeipoor-Anari. *J. Magnet. Magnt. Mat,* 2016, **398**, 205.

19 M. Nasr-Esfahani, S. Jafar Hoseini, M. Montazerozohori, R. Mehrabi, H. Nasrabadi. *J. Mol. Catal. A Chemical.* 2014, **382**, 99.

20 P. Murthy, D. Rambabu, G. R. Krishna, C. M. Reddy, K. R. S. Prasad, M. V. Basaveswara Rao, M. Pal, *Tetrahedron Lett.* 2012, **53**, 863.

21 B. Vilas Labade, V. Pravin Shinde, S. Murlidhar Shingare, *Tetrahedron Lett.* 2013, **54**, 5778.

22 S. Kumar, P. Sharma, K. K. Kapoor, M. Singh Hundal, *Tetrahedron* 2008, **64**, 536.

23 B. V. Subba Reddy, A. Venkateswarlu, C. Madan, A. Vinu. *Tetrahedron Lett*. 2011, **52**, 1891.

24 M. Thimmaiah, P. Li, S. Regati, B. Chen, J. Cong-Gui Zhao, *Tetrahedron Lett.* 2012, **53**, 4870.

25 S. Ray, C. Mukhopadhyay, *Lett. Appl. Nano BioScience*, 2014, **3**, 220.

26 P. Manna, P. K. Maiti, *Tetrahedron Lett.* 2015, **56**, 5094.

27 P. V. Shinde, S. S. Sonar, B. B. Shingate, M. S. Shingare, Tetrahedron Lett. 2010, **51**, 1309.

28 J. Safaei-Ghomi, M. A. Ghasemzadeha, M. Mehrabib, *Scientia Iranica C,* 2013, **20**, 549.

29 A. Molla, S. Hussain, S. Affiliations, *RSC Adv.* 2014, **4**, 29750.

30 A. Ghorbani-Choghamarani, M. Norouzi, *J. Mol. Catal. A Chemical,* 2014, **395**, 172-179.

31 A. Ghorbani-Choghamarani, Z. Darvishnejad, M. Norouzi, *Appl. Organometal. Chem.* 2015, **29**, 707.

32 A. Ghorbani-Choghamarani, G. Azadi, *RSC Adv.* 2015, **5** 9752.

33 M. Ghorbani-Choghamarani, M. Hajjami, M. Norouzi, Y. Abbasityula, V. Eigner, M.Dusek, *Tetrahedron*, 2013, **69**, 6541.

34 Ghorbani-Choghamarani, M. Norouzi, *Lett. Org. Chem.* 2013, **10**, 562.

35 A. Ghorbani-Choghamarani, B. Tahmasbi, *New J. Chem.***,** 2016, **40**, 1205.

View Article Online
DOI: 10.1039/C6RA19776K

Graphical abstract

Heterogeneous Cu(II)/L-His@Fe_3O_4 nanocatalyst: a novel, efficient and magnetically-recoverable catalysts for organic transformations in green solvents

Masoomeh Norouzi, Arash Ghorbani-Choghamarani,* Mohsen Nikoorazm